# Highly Accurate Extrinsic Calibration of Terrestrial Laser Scanner and Digital Camera for Structural Monitoring Applications

Mohammad Omidalizarandi*, Jens-André Paffenholz, Ulrich Stenz, Ingo Neumann
Geodetic Institute
Leibniz Universität Hannover, Nienburger Str. 1, 30167, Hannover, Germany
{zarandi, paffenholz, stenz, neumann}@gih.uni-hannover.de

**Abstract.** In the current state-of-the-art, monitoring and analysis of short- and long-term deformations of natural and artificial objects (e.g. dams, bridges, towers, landslides,...) has received increasing interest by researchers and operators who are involved in this field of Geodetic science and engineering. In order to improve the accuracy of deformation monitoring and analysis, terrestrial laser scanner (TLS) and high resolution digital camera are integrated to optimally combine their information. TLS can directly provide 3D spatial coordinates of the object surface in combination with reflectivity values. In addition, digital cameras can acquire high resolution images. The information from both camera and TLS are complementary to each other. The strength of one measurement method overcomes the weakness of the other one.

In order to fuse the acquired data from these two kinds of sensors in the common coordinate system, it is a vital and pre-requisite step to precisely determine the extrinsic parameters between TLS and digital camera. Thus, the calibration of the aforementioned hybrid sensor system can be separated into three single calibrations: calibration of the camera, calibration of the TLS and extrinsic calibration between TLS and digital camera. Camera calibration and TLS calibration (internal error sources) are commonly performed in advance in a 3D laboratory.

In this research, we focus on the high accurate estimation of extrinsic parameters between fused sensors on the basis of target-based calibration using different types of observations (image measurements, TLS measurements and laser tracker measurements for validation) by considering different weights. Space resection bundle adjustment is solved based upon Gauss-Markov and Gauss-Helmert model. At the end, three case studies are investigated in the 3D laboratory and numerical results of the aforementioned calibration are presented and discussed. The results depict that high accurate extrinsic parameters are achieved with applied Gauss-Helmert model and variance component estimation in the integrated multi-sensor-system. Finally, a real world case study of a selected structural monitoring project is presented and discussed.

**Keywords.** Terrestrial Laser Scanner, Digital Camera, Multi-Sensor-System, Extrinsic Calibration, Deformation Analysis

## 1 Introduction

Today, monitoring and analysis of short- and long-term deformations of natural and artificial objects (e.g. dams, bridges, towers, landslides,...) has received increasing interest both in Geodetic science and engineering applications. In this work, integration of TLS (here the Zoller+Fröhlich IMAGER 5006) and high resolution digital camera (here NIKON D750) affords increasing the accuracy of deformation monitoring and analysis by high accurately estimation of the extrinsic parameters between fused sensors as preliminary stage. TLS can directly provide fast and reliable 3D spatial coordinates of the object surface in combination with reflectivity values. In addition, digital cameras can acquire high resolution images with high quality colour information. In the combined sensor system, high resolution cameras are beneficial due to having high angular accuracy of sub-pixel accuracy image measurements which would improve the lateral accuracy of laser scanners (Schneider and Maas (2007)). On the other hand, combination of TLS and digital camera is worthwhile due to increasing the redundancy in the adjustment procedure. In addition, in case of large incidence angle of the TLS, digital images are more advantageous in deformation analysis of artificial objects. Furthermore, by the usage of digital

* Corresponding author.

peer JISDM 2016 Vienna reviewed

images, deformation analysis in both direction of laser beam and perpendicular to laser beam is possible.

In this specific study, the digital camera is rigidly mounted on top of the TLS by the usage of a clamping system (figure 1 (left)). To avoid any vibration of camera and blurring of images, Nikon wireless mobile utility application is setup on the cell phone and images are taken indirectly. Mounting a digital camera externally on the top of the scanner has an advantage of flexibility of the used sensors. (e.g. cameras with a different resolution or focal length) (Wendt and Dold (2005)). As a drawback, in case of disconnecting clamping system for transportation, calibration should be performed for each mount. In order to overcome this problem, Omidalizarandi and Neumann (2015) applied mutual information based calibration for in situ calibration which is based upon adaption of Pandey's work (Pandey et al. (2012)) to the integrated system of TLS and camera and results seem promising.

**Fig. 1** A Nikon D750 24.3-megapixel digital camera is rigidly mounted on top of the Z+F Imager 5006 TLS (left), Leica AT901LR LT (right)

This paper addresses the topic of high accurate extrinsic calibration of terrestrial laser scanner and digital camera for structural monitoring applications. Under this approach, focal length of the camera, exterior orientation parameters between TLS and camera, exterior orientation parameters between TLS and laser tracker (LT (figure 1 (right))) and target coordinates are estimated with high accuracy. LT as an additional sensor allows extreme accuracy of the target points (Positional accuracy of 15 µm + 6 µm/m (Leica Geosystems, PCMM system specifications (2010)) and can be considered as a reference coordinate frame. In addition, its measurements are performed independently from the integrated sensor system.

In the multi-sensor-system, estimation of extrinsic calibration parameters between fused sensors is an important and preliminary procedure to obtain geometric transformation parameters between different sensors and to relate acquired data. The extrinsic calibration parameters between digital camera and TLS, six degree of freedom (6 DOF), are the position and orientation of the digital camera relative to TLS, that is identifying the rigid body transformation from the digital camera coordinate system to the TLS coordinate system. Extrinsic calibration parameters between TLS and LT, seven degree of freedom (7 DOF), are the scale, position and orientation of the TLS with respect to LT that is so called similarity transformation. The rigid body transformation allows re-projection of the 3D point clouds from the TLS coordinate system to the 2D camera coordinate system.

Zhang and Pless (2004) proposed an algorithm to estimate extrinsic calibration parameters between camera and 2D laser range finder (LRF) using planar checkerboard pattern to match laser scan line on the planar pattern with the pattern plane from the camera image. Thereafter, global optimization method is applied to refine the parameters. Lichti et al. (2010) described the method for self-calibration of integrated range camera system to simultaneously estimate camera calibration parameters and rangefinder systematic error parameters in a free-network bundle adjustment using signalised targets. Its mathematical concept is collinearity equations and range observation equations. Variance component estimation (VCE) is applied to iteratively re-weight observations optimally. Schneider and Maas (2007) proposed an algorithm to combine TLS data, central perspective and panoramic images in the integrated bundle adjustment using Gauss-Markov model with applied VCE as well. Object points coordinates, interior and exterior orientation parameters of the sensors are computed as unknown parameters. In addition, aforementioned parameters are evaluated with statistical test. Pandey et al. (2012) proposed the automatic targetless extrinsic calibration of a 3D laser scanner and camera system based upon mutual information (MI) algorithm and estimating calibration parameters by maximizing the mutual information between the reflectivity values of the laser scanner and intensity values of the camera

image. Afterwards, gradient ascent algorithm is applied to consider different scans from different scenes in a single optimization framework. As a drawback of this approach, it is not applicable for 3D point clouds without reflectivity information. In addition, it needs quite good initialization values of the 6 DOF. Mirzaei et al. (2012) proposed the algorithm to estimate the intrinsic and extrinsic calibration parameters of a 3D LIDAR and rigidly connected camera in two least square sub-problems using measurements of a calibration plane at various configurations.

The innovation of the implemented algorithm comparing to the proposed approach of Schneider and Maas (2007) is related to utilizing LT measurements as an additional observation to increase the redundancy and accuracy as a reference coordinate system. In addition, by the usage of LT, validation of the extrinsic parameters between TLS and digital camera is performable. Due to the usage of different sensors and different calibration laboratory, it is quite hard to discuss or compare results of two approaches together. However, authors believe that could achieve very high accurate extrinsic parameters between TLS and digital camera which is the preliminary stage for deformation analysis in the further steps.

## 2 Data Acquisition, Interfacing and Pre-Processing

The data acquisition step consists of acquiring image measurements, TLS measurements and LT measurements.

TLS data are acquired in "super high" resolution mode with normal quality. The vertical and horizontal resolution is $0.0018^{\circ}$ and vertical and horizontal accuracy is $0.007^{\circ}$ rms (IMAGER 5006, Technical Data). In addition, TLS point targets accurately extracted using "Fit target" mode of the Z+F LaserControl software. As can be seen from figure 2 (left), back of the target consists of hemisphere metal staff which fits precisely to the magnetic holder (figure 2 (middle-left)).

Image measurements are performed using sub-pixel target mode of the PhotoModeler software. As depicted in figure 2 (middle-right), four centroids of the circles in each target are measured and center of the target is computed on the basis of the averaging of the measured centroids. In addition, the pixel resolution of the digital images in the large mode image size is approximately 0.00597 (Nikon D750, User's Manual (2014)).

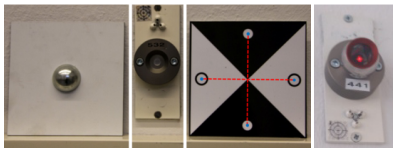

**Fig. 2** Back of the target(left), magnetic holder (middle-left) and front of the target with depiction of detected centroid of circles using PhotoModeler software (middle-right), mounted corner cube reflector at the magnetic holder (right)

In order to measure target point with very high accuracy, LT is utilized as an additional sensor and it is pointed to the mounted corner cubes reflector at the magnetic holder (figure 2 (right)).

The horizontal angle measurement of the TLS (Az) is defined by a 3x3 rotation matrix to rotate TLS data around its Z-axis at the time of exposure (Al-Manasir and Fraser (2006)). It is important for rotating 3D point clouds from TLS coordinate frame to the digital camera coordinate frame as depicted in figure 3. Thus, it is written down for each image to be considered as additional observation in the adjustment procedure.

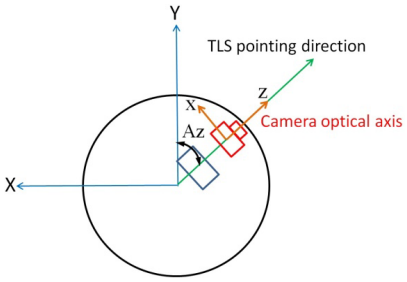


**Fig. 3** The TLS and camera coordinate systems from the top view

## 3 Methodology

In this research, camera calibration and extrinsic calibration of TLS and camera are carried out respectively. TLS calibration is skipped since we assumed that TLS has been calibrated in advance in our 3D laboratory. It would be taken into the account in the future for in situ calibration to achieve more precise and accurate results.

### 3.1 Mathematical Models

In the first step, interior orientation parameters of the camera consisting of principal point $(x_p, y_p)$, focal length (f), coefficients of radial distortion

$(K_1, K_2, K_3)$ and coefficients of decentering distortion $(P_1, P_2, P_3)$ are determined in laboratory using PhotoModeler software. Thereafter, according to Brown's equations (1971), (x,y) which are image measurements are rectified to $(x', y')$ which are rectified image measurements as:

$$x' = x + \bar{x}(K_1 r^2 + K_2 r^4 + K_3 r^6 + \cdots) + (P_1(r^2 + 2\bar{x}^2) + 2P_2 \bar{x}\bar{y}) \quad (1)$$

$$y' = y + \bar{y}(K_1 r^2 + K_2 r^4 + K_3 r^6 + \cdots) + (P_2(r^2 + 2\bar{y}^2) + 2P_1 \bar{x}\bar{y}) \quad (2)$$

where

$$\bar{x} = x - x_p \quad (3)$$

$$\bar{y} = y - y_p \quad (4)$$

$$r = \sqrt{\left[(x - x_p)^2 + (y - y_p)^2\right]} \quad (5)$$

In the next step, TLS's exterior orientation parameters with respect to the camera coordinate system, TLS's exterior orientation parameters with respect to the LT coordinate system and focal length of the camera are determined. The mathematical model to compute extrinsic parameters between TLS and digital camera (equation 10) is determined based upon collinearity equations and is solved by space resection bundle adjustment (Al-Manasir and Fraser (2006)). The mathematical model to compute extrinsic parameters between TLS and LT is on the basis of similarity transformation. Due to non linear collinearity equations or similarity transformation for the least-squares solution, linearization should be performed. Thus, initial starting values are estimated using direct linear transform (DLT) in combination with RANSAC algorithm to robustly estimate the parameters.

Least-square solutions can be achieved by Gauss-Markov model (GM) or Gauss-Helmert model (GH). Thus, four target functions (equations 6-9) are determined.

$$F_x = x - f\frac{r}{q} \quad (6)$$

$$F_y = y - f\frac{s}{q} \quad (7)$$

$$F = \lambda \boldsymbol{R}_{\kappa'\varphi'\omega'} \begin{bmatrix} X_{TLS} \\ Y_{TLS} \\ Z_{TLS} \end{bmatrix} + \begin{bmatrix} X_c' \\ Y_c' \\ Z_c' \end{bmatrix} - \begin{bmatrix} X_L \\ Y_L \\ Z_L \end{bmatrix} \quad (8)$$

$$F = \begin{bmatrix} X \\ Y \\ Z \end{bmatrix} - \begin{bmatrix} X_{TLS} \\ Y_{TLS} \\ Z_{TLS} \end{bmatrix} \quad (9)$$

where

$$\begin{bmatrix} r \\ s \\ q \end{bmatrix} = \boldsymbol{R}_{\kappa\varphi\omega} * \left[ \boldsymbol{R}_3(Az) \begin{bmatrix} X_{TLS} \\ Y_{TLS} \\ Z_{TLS} \end{bmatrix} - \begin{bmatrix} X_c \\ Y_c \\ Z_c \end{bmatrix} \right] \quad (10)$$

In equations (6-10), $(x, y)$ are the target coordinates in the image space, $(X, Y, Z)$ are the target coordinates in the object space, $(X_{TLS}, Y_{TLS}, Z_{TLS})$ are TLS point coordinates of the targets, $(X_C, Y_C, Z_C)$ are the translations vector between TLS and digital camera, $(\kappa, \varphi, \omega)$ are the rotation angles between TLS and digital camera, (Az) is horizontal angle measurement of the TLS, $(X_C', Y_C', Z_C')$ are the translations vector between TLS and LT, $(X_L, Y_L, Z_L)$ are LT point coordinates of the targets, $(\kappa', \varphi', \omega')$ are the rotation angles between TLS and LT and $(\lambda)$ is the scale factor between TLS and LT. Equations (6) and (7) are collinearity equations to transfer TLS coordinate system to digital camera coordinate system. Equation (8) is similarity transformation to transfer TLS coordinate system to LT coordinate system and equation (9) is constraint to compute target point coordinates in the object space. For further information concerning DLT algorithm, collinearity equations and rotation angle matrices, please refer to, e.g., Luhmann et al. (2006).

GM model is a set up linear or non linear relation between observations and unknown parameters. It is solely defined by observations and estimates unknown parameters. In this type of adjustment model for our research, square sum of residuals are minimized merely for one type of observation (Image measurements). GH model (mixed model) is the more complete and sophisticated model compared to GM model and as its privilege, all the unknown parameters and observations can be updated as unknown in the iterative procedure and this proceeds till they satisfy the predefined criterion. For further information concerning Gauss-Markov model and Gauss-Helmert model, please refer to the, e.g., Niemeier (2002).

### 3.2 Statistical Test and Variance Component Estimation

The statistical test is performed to interpret the adjustment results and to evaluate the uncertainty of the measurements and unknown parameters. In addition, it is appropriate to identify gross errors in the observations and consequently exclude them from the solutions (Schneider (2008)). In this research, $\chi^2$ test with 95% confidence level is applied. If the statistical test result is greater than

predetermined limit, the null hypothesis is rejected and it means that observations are not normally distributed. The $\chi^2$ test for all measurements is performed based on equation (11).

$$\chi^2 \sim \frac{v^T P v}{\sigma_0^2} \quad (11)$$

In the above equation, $v$ stands for a few residuals of the measurements. In addition, residuals of each type of observations (e.g. image measurements and so on) are separated and considered individually.

The test is performed for each type of observations to investigate the adjustment results. In the next step, the local test for each measurement is carried out to reject outliers. This procedure proceeds till no measurements remain to be rejected.

In the combined sensor system, due to simultaneously utilizing different types of observations with different geometric and stochastic models in the adjustment procedure, adequate weights have to be assigned to the measurements. Thus, VCE is applied in the integrated bundle adjustment to automatically determine optimal observation weights to exploit the potential of the fused sensor data completely (Schneider (2008)).

## 4 Experimental Results

In this research, two different adjustment models in three different case studies are investigated separately. The size of 3D laboratory is 6.2 m (width) * 8.6 m (length) * 4.9 m (height) and it is measured with Z+F IMAGER 5006 in the super high resolution mode with horizontal and vertical angle resolution of $0.0018^{\circ}$. Afterwards, 16 images are taken with Nikon D750 which fully covers our 3D laboratory with all existing targets. Targets are randomly distributed on the walls, ceiling and floor and are measured in the image space and object space, respectively. The number of measured targets in object space is 25 and number of measured targets in the image space is 88 due to overlapping of the images. Thereafter, targets are measured one by one with LT to validate and check the accuracy of our calibration results. At the end, a real world case study of a selected structural monitoring project is presented and discussed.

### 4.1 Case Study I - GM Model

In the first case study, GM model is implemented for the least-square solution. Applied sensors are TLS and digital camera. Extrinsic parameters between TLS and digital camera (translations and rotations (6 DOF)) and focal length of the camera (f) are the unknown parameters that are depicted in the table 1.

**Table 1.** Extrinsic parameters between TLS and digital camera (6 DOF) plus focal length with applied GM model

| 6 DOF | Value | σ |
|---|---|---|
| $\omega$ | 88.7154 (Degree) | 0.0059 |
| $\varphi$ | 0.0903 (Degree) | 0.0064 |
| $\kappa$ | 0.0420 (Degree) | 0.0033 |
| $X_C$ | 0.0001 (m) | 0.0004 |
| $Y_C$ | 0.2193 (m) | 0.0004 |
| $Z_C$ | 0.0930 (m) | 0.0011 |
| f | 20.6206 (mm) | 0.0001 |

VCE is applied additionally to estimate standard deviation of the image measurements iteratively and optimally. Due to applying VCE merely for one type of the observation (image measurements), a-posteriori variance factor of unit weight ($\hat{\sigma}_0^2$) yields the same result as VCE which is equal to 0.0045.

### 4.2 Case Study II - GH Model

In the second case study, least square solution is solved for TLS and digital camera with applied GH model. Observations are target coordinates in the image space, TLS coordinates of the targets and horizontal angle of TLS. Extrinsic parameters between TLS and digital camera (6 DOF) and focal length of the camera (f) are the unknown parameters that are depicted in the table 2. In this case study, VCE is applied for image measurements, TLS measurements and horizontal angle measurement of TLS.

**Table 2.** Extrinsic parameters between TLS and digital camera (6 DOF) plus focal length with applied GH model

| 6 DOF | Value | σ |
|---|---|---|
| $\omega$ | 88.7239 (Degree) | 0.0054 |
| $\varphi$ | 0.1030 (Degree) | 0.0075 |
| $\kappa$ | 0.0433 (Degree) | 0.0029 |
| $X_C$ | -0.0008 (m) | 0.0005 |
| $Y_C$ | 0.2199 (m) | 0.0004 |
| $Z_C$ | 0.0955 (m) | 0.0011 |
| f | 20.6058 (mm) | 0.0062 |

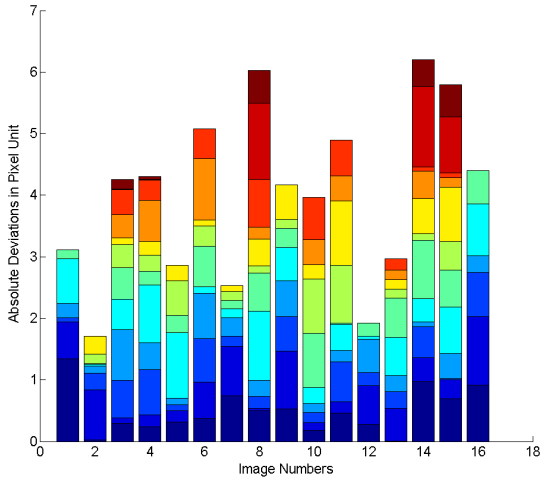


**Fig. 4** Absolute deviations of the estimated image targets and image targets measurements in pixel unit

Figure 4 depicts the absolute deviations of the estimated image targets and image targets measurements in pixel unit. X-axis corresponds to image numbers and Y-axis corresponds to absolute deviations in pixel unit. For each image, all the targets with their deviations in x and y directions are taken into account in one column. For instance, in the first column of the figure 4, image one contains three targets which with consideration of their deviations in x and y directions respectively, six colourful blocks are shown and so on. This case study is performed for 16 images. As can be seen from the results, for some images absolute deviations are less than others which is related to the less number of targets in those images.

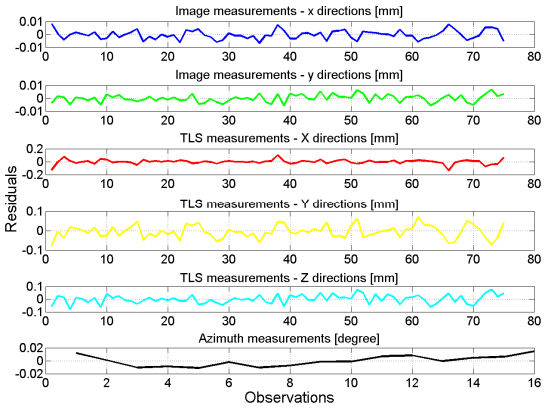


**Fig. 5** Residuals of the observations

Figure 5 depicts the residuals for all type of the observations. From top, first and second graphs, are image measurements residuals in x and y directions. Third to fifth graphs are TLS measurements residuals in X, Y and Z directions. The sixth graph is residuals of horizontal angle measurement of TLS.

Results of the VCE are illustrated in table 3. Furthermore, a-posteriori variance factor of unit weight ($\hat{\sigma}_0^2$) is computed for entire measurements that is equal to 0.92307. The standard deviations before adjustments are equal to nominal or expected standard deviations of the observations. Standard deviations after adjustment are the result of VCE. Furthermore, standard deviation of TLS measurements yields better accuracy than prior expected value.

**Table 3.** Standard deviations of the observations

| Observations | $\sigma$ - before adjustment | $\sigma$ - after adjustment |
|---|---|---|
| Image (mm) | 0.006 | 0.0037 |
| TLS (mm) | 1.0 | 0.1747 |
| Az (Degree) | 0.007 | 0.0087 |

### 4.3 Case Study III - Validation

In the third case study, GH model is implemented for the least-square solution. Applied sensors are TLS, LT and digital camera. Observations are target coordinates in the image space, TLS coordinates of the targets, LT coordinates of the targets and horizontal angle measurements of TLS. Extrinsic parameters between TLS and digital camera (table 4), extrinsic parameters between TLS and LT (table 5), focal length and target point coordinates in object space are the unknown parameters. Furthermore, VCE is applied additionally for all type of the observations.

**Table 4.** Extrinsic parameters between TLS and digital camera (6 DOF) with applied GH model

| 6 DOF | Value | σ |
|---|---|---|
| $\omega$ | 88.7251 (Degree) | 0.0060 |
| $\varphi$ | 0.1231 (Degree) | 0.0092 |
| $\kappa$ | 0.0444 (Degree) | 0.0032 |
| $X_C$ | -0.0025 (m) | 0.0007 |
| $Y_C$ | 0.2199 (m) | 0.0004 |
| $Z_C$ | 0.0953 (m) | 0.0002 |

**Table 5.** Extrinsic parameters between TLS and LT (7 DOF) with applied GH model

| 7 DOF | Value | σ |
|---|---|---|
| $\omega'$ | 0.1048 (Degree) | 0.0010 |
| $\varphi'$ | -0.0621 (Degree) | 0.0015 |
| $\kappa'$ | 96.3564 (Degree) | 0.0011 |
| $X_C'$ | 12.8279 (m) | 0.0001 |
| $Y_C'$ | 13.9029 (m) | 0.0001 |
| $Z_C'$ | 1.6953 (m) | 0.0001 |
| $\lambda$ | 0.9999 | 0.0001 |

Figure 6 depicts the residuals for all type of the observations and figure 7 depicts the absolute deviations of the estimated image targets and image targets measurements in pixel unit.

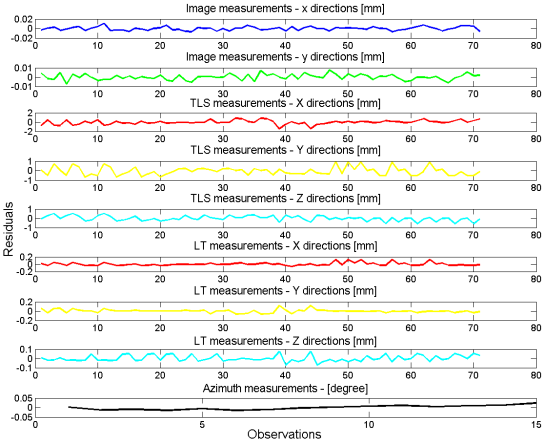


**Fig. 6** Residuals of the observations

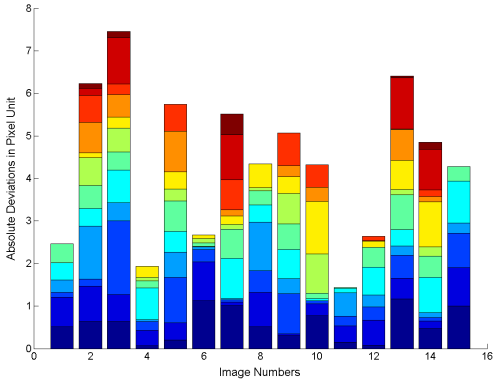


**Fig. 7** Absolute deviations of the estimated image targets and image targets measurements in pixel unit

Results of the variance component estimation are illustrated in table 6. Furthermore, a-posteriori variance factor of unit weight ($\hat{\sigma}_0^2$) is computed for entire measurements that is equal to 0.9087. Standard deviations after adjustment which are results of VCE are not significant comparing to the standard deviations before adjustment except of horizontal angle measurement of TLS which is slightly greater than expected value.

**Table 6.** Standard deviations of the observations

| Observations | | $\sigma$ - before adjustment | $\sigma$ - after adjustment |
|---|---|---|---|
| Image | (mm) | 0.006 | 0.0040 |
| TLS | (mm) | 1.0 | 0.4653 |
| LT | (mm) | 0.1 | 0.1091 |
| Az | (Degree) | 0.007 | 0.01197 |

**Fig. 8** Scheme of calibration room (left) and the magnification of one of the targets. (Red dot: initial value, Blue dot: image measurements, Green dot: re-projected TLS data to image space, Yellow dot: estimated image measurements)

Figure 8 depicts the initialization and estimated measurement for one of the target in our 3D laboratory. Thus, figures 4 and 7 are comparison of the yellow dots vs. blue dots.

### 4.4 Case Study IV - Real World Application

In the fourth case study, the applicability of our proposed approach is investigated in an outdoor environment. The outdoor experiment took place in the vicinity of Freyburg, Germany. The goal is to detect the deformation of a gabion, which is characterized by a wire mesh frame which is filled with stones (figure 9 (top)). The aforementioned object was measured with the multi-sensor-system of TLS and rigidly attached digital camera. In order to make this data fusion more visible, downsampling of the Point Cloud Library (PCL) is applied. As can be seen from figure 9 (bottom), TLS data downsampled and re-projected to the rectified RGB image. Re-projection is performed by the concept of central perspective approach based

upon collinearity equation (Moussa et al., 2012). In the next step, wire mesh frames of the RGB image are extracted using edge detection algorithm which yields determination of the intersections of the lines as interest points in image space. Thereafter, due to one to one relationship between TLS data and RGB image, deformation in both directions of laser beam and perpendicular to laser beam is detectable.

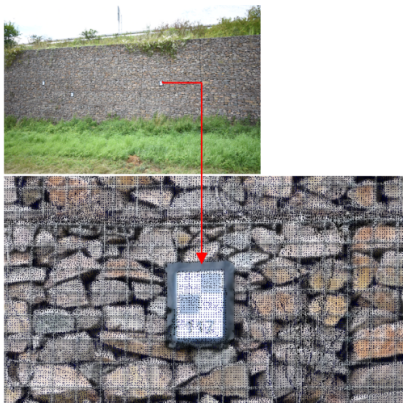

**Fig. 9** Depiction of gabion made of wire mesh frames filled with stones near Freyburg, Germany (top), magnified re-projection of downsampled point clouds into the rectified RGB image based upon estimated extrinsic calibration parameters of the 3D laboratory (bottom)

## Conclusion

The main objective of this research is to determine extrinsic parameters between fused sensors (TLS, digital camera and LT). Three case studies with two different adjustment models are applied. The results depict that high accurate extrinsic parameters between TLS and digital camera are achieved with applied GH model and VCE in the integrated multi-sensor-system. Additionally, final standard deviations of the observations have minor differences with nominal or expected standard deviations of the observations before adjustment which prove the correctness and accuracy of implemented algorithm. In addition, combination of GH model and VCE yields high accurate estimation of standard deviations for all type of the observations at once. In addition, LT measurements are utilized as an additional observation to validate the final results.

In the future work, interest points of the wire mesh frames are extracted in both object space and image space to be able to perform more accurate deformation analysis.

## References


Al-Manasir, K., & Fraser, C. S. (2006). Registration of terrestrial laser scanner data using imagery. *The Photogrammetric Record*, 21(115), 255-268.

Duane, C. Brown. (1971). Close-range camera calibration. *Photogram. Eng. Remote Sens*, 37, 855-866.

Leica Geosystems (2010). PCMM system specifications, Leica absolute tracker and Leica T-products.

Lichti, D. D., Kim, C., & Jamtsho, S. (2010). An integrated bundle adjustment approach to range camera geometric self-calibration. *ISPRS Journal of Photogrammetry and Remote Sensing*, 65(4), 360-368.

Luhmann, T., Robson, S., Kyle, S., & Harley, I. (2006). Close range photogrammetry: Principles, methods and applications (pp. 1-510). Whittles.

Mirzaei, F. M., Kottas, D. G., & Roumeliotis, S. I. (2012). 3D LIDAR–camera intrinsic and extrinsic calibration: Identifiability and analytical least-squares-based initialization. *The International Journal of Robotics Research*, 31(4), 452-467.

Moussa, W., Abdel-Wahab, M., & Fritsch, D. (2012). An Automatic Procedure for Combining Digital Images and Laser Scanner Data. *International Archives of the Photogrammetry, Remote Sensing and Spatial Information Sciences*, 39, B5.

Niemeier, W. (2002). Ausgleichungsrechnung: eine Einführung für Studierende und Praktiker des Vermessungs-und Geoinformationswesens. Walter de Gruyter, Berlin.

Nikon, Digital Camera D750, User's Manual (2014).

Omidalizarandi, M. & Neumann, I. (2015). Comparison of Target- and Mutual Information based Calibration of Terrestrial Laser Scanner and Digital Camera for Deformation Monitoring. *The International Archives of Photogrammetry, Remote Sensing and Spatial Information Sciences*, *40*(1), 559.

Pandey, G., McBride, J. R., Savarese, S., & Eustice, R. (2012). Automatic Targetless Extrinsic Calibration of a 3D Lidar and Camera by Maximizing Mutual Information. *Proceedings of the AAAI National Conference on Artificial Intelligence*, pp. 2054-2056.

Schneider, D., & Maas, H. G. (2007). Integrated bundle adjustment of terrestrial laser scanner data and image data with variance component estimation. *The Photogrammetric Journal of Finland*, *20*, 5-15.

Schneider, D. (2008). Geometrische und stochastische Modelle für die integrierte Auswertung terrestrischer Laserscannerdaten und photogrammetrischer Bilddaten. Available from: http://dgk.badw.de/fileadmin/docs/c-642.pdf

Wendt, A., & Dold, C. (2005). Estimation of interior orientation and eccentricity parameters of a hybrid imaging and laser scanning sensor. *Proceedings of the ISPRS working group*, *5*, 1682-1750.

Zhang, Q., & Pless, R. (2004). Extrinsic calibration of a camera and laser range finder (improves camera calibration). In *Intelligent Robots and Systems, 2004,(IROS 2004). Proceedings. 2004 IEEE/RSJ International Conference on* IEEE (Vol. 3, pp. 2301-2306).